Modeling the Electrophoresis of Rigid Polyions. Inclusion of Ion Relaxation

Stuart A. Allison

Department of Chemistry, Georgia State University, Atlanta, Georgia 30303

Received June 19, 1996; Revised Manuscript Received August 14, 1996[⊗]

ABSTRACT: A numerical algorithm is developed to calculate electrophoretic mobilities of rigid model polyions that includes the effect of ion relaxation. The Navier−Stokes, Poisson, and ion transport equations are cast into forms that are amenable to numerical solution by boundary element procedures. The three equations are solved simultaneously by an iterative procedure. It is applied first to a spherical polyion containing a centrosymmetric charge distribution and double layer that is not thin compared to the radius of the sphere. Resulting mobilities compare favorably (to within 10%) with independent theory. The algorithm is then applied to spherical polyions containing noncentrosymmetric charge distributions. Although the present calculations are restricted to spherical polyions, there is no formal difficulty in extending them to nonspherical polyions.

Introduction

Electrophoresis continues to be a very useful and powerful technique in the separation and characterization of biomolecules and colloids. In its simplest form (free solution electrophoresis), a dilute suspension of charged particles (colloids or macromolecules) is subjected to a constant external electric field and the particle translates through the solution with some steady state velocity. The electrophoretic mobility (ratio of steady state velocity to applied field strength) depends in a complex way on the charge, size, and shape of the particle as well as the solvent, nature of co-ions and counterions present, and perhaps the field strength. There exists an extensive literature on the theory of electrophoresis, as summarized in a number of excellent reviews.[1−4] Of all the theories, those restricted to thin double layers in the absence[5,6] or presence[7,8] of ion relaxation are the most thoroughly developed. Ion relaxation refers to the perturbation of the ion atmosphere in the vicinity of the particle in response to the imposed electric and flow fields. The double layer refers to that layer of fluid surrounding the particle over which the local ion concentration deviates significantly from its ambient value and can be equated roughly to κ^{-1} where κ is the Debye−Huckel screening parameter. The double layer is considered to be "thin" if κ^{-1} is small compared to the smallest linear dimension of the particle. For a 0.1 M NaCl solution, κ^{-1} is about 1 nm and the thin double layer theories can be applied to globular particles in the 10 nm size range or larger, such as colloidal latex particles.[9] However, many polyions of biological interest are much smaller than this and these systems require theories that account for the double layer thickness relative to the particle size and shape. In this work, we shall be primarily interested in the case where the double layer is not thin.

The theories of electrophoresis of spherical particles containing centrosymmetric charge distributions and double layers of arbitrary thickness have been developed in both the absence[10] and presence[11−15] of ion relaxation. Whether or not ion relaxation is important in this case (sphere containing a centrosymmetric charge distribution) depends on the polyion charge or surface potential, size, salt concentration and valency of its constituent ions, and the ion mobilities. A fairly useful rule of thumb is that if the reduced surface potential (actual potential times protonic charge divided by k_BT) exceeds 2, ion relaxation will be important.[14] On this basis, we would expect ion relaxation to be important for DNA[16] but not for typical proteins on the basis of their comparably low net charge.[17] However, this conclusion is only tentative since it is based on simple spherical models. Actual proteins are nonspherical and contain complex charge distributions that may produce localized regions of high absolute electrostatic potential in the fluid domain, as illustrated by superoxide dismutase.[18] Whether or not ion relaxation is important in protein electrophoresis is a question that merits further study.

The objective of the present work is to develop a method of determining the electrophoretic mobility of rigid polyions of arbitrary shape and charge distribution which also accounts for ion relaxation. It extends previous work which left ion relaxation out[17,19] or included it,[20] but only for a spherical polyion with a central charge. The polyion is represented as a low dielectric volume element enclosed by a molecular surface made of a series of flat triangular platelets. Outside the molecular surface is the solvent continuum characterized by a dielectric constant different from that of the polyion. Including ion relaxation complicates the problem substantially because of the coupling of the fluid flow, ion densities, and external electric and/or flow fields.[11−15] This requires simultaneous solution of the Navier−Stokes, Poisson, and ion transport equations. In the present work, we accomplish this by using boundary element methods to solve the three equations simultaneously. The algorithm is first applied to a spherical polyion containing a single central charge to confirm it is working correctly. Then it is applied to spherical polyions containing a variety of noncentrosymmetric charge distributions.

Determining the Electrophoretic Mobility

The computational strategy of determining electrophoretic mobility when ion relaxation is included is similar to that employed previously in the absence of relaxation[17] so only an outline shall be presented here. The key quantity required is the total force, **z**, on the polyion which is the sum of electrostatic and hydrodynamic components. Consider a polyion translating through a viscous, incompressible fluid with velocity **u**.

[⊗] Abstract published in *Advance ACS Abstracts,* October 1, 1996.

S0024-9297(96)00890-X CCC: $12.00

It is assumed the fluid is at rest far from the polyion. The jth component of the force can be computed by a Teubner relation[21]

$$z_j = \mathbf{u}\cdot\mathbf{z}_{h0}^{(j)} + \int_V [\mathbf{v}^{(j)}(\mathbf{x}) - \mathbf{i}_j]\cdot\mathbf{s}(\mathbf{x})\, dV_x \quad (1)$$

where $\mathbf{z}_{h0}^{(j)}$ is the hydrodynamic force on the corresponding uncharged polyion translating with unit velocity in direction j, $\mathbf{v}^{(j)}(\mathbf{x})$ is the fluid velocity at $\mathbf{x}$ that is due to the translation of the equivalent uncharged polyion translating with unit velocity in the direction j, $\mathbf{i}_j$ is a unit vector along j, and $\mathbf{s}(\mathbf{x})$ is the external force per unit volume on the fluid at $\mathbf{x}$. The calculation of the hydrodynamic force and fluid velocity for the uncharged polyion are computed by the boundary element method for the special case $\mathbf{s}(\mathbf{x}) = 0$. In this work, the external force, $\mathbf{s}$, is assumed to arise from the various electrostatic interactions that are present. If Λ is the total electrostatic potential and ρ is the charge density, then

$$\mathbf{s}(\mathbf{x}) = -\rho(\mathbf{x})\nabla\Lambda(\mathbf{x}) \quad (2)$$

In order to determine the total force on the polyion, it is necessary to first determine the electrostatic potential and ion densities. This, in turn, requires simultaneous solution of the Poisson and ion transport equations.[11−15,20] As discussed previously, in many applications it is a good approximation to neglect ion relaxation. In previous work,[17] the BE method was applied to the electrophoretic mobility of arbitrary rigid polyions with ion relaxation ignored. In the present work, the "no relaxation" limit serves as a starting estimate for the more general problem. The determination of Λ and ρ are discussed in the next section.

Following O'Brien and White,[15] it is useful to consider two distinct transport cases. In the transport 1 (T1) case, no external electric field, $\mathbf{e}$, is present, but the polyion is translated with velocity $\mathbf{u}$ through an unbounded fluid that is stationary far away from the polyion. The total force, $\mathbf{z}(1)$, on the polyion can be written[17]

$$\mathbf{z}(1) = -\eta\mathbf{K}\cdot\mathbf{u} \quad (3)$$

where $\mathbf{K}$ is the translational friction tensor and η is the fluid viscosity. The components of $\mathbf{K}$ are readily obtained by translating the model polyion along a single axis and computing the force components using eq 1. In the transport 2 (T2) case, the polyion is held stationary in a constant external electric field, $\mathbf{e}$. The total force, $\mathbf{z}(2)$, is given by

$$\mathbf{z}(2) = \eta\mathbf{Q}\cdot\mathbf{e} \quad (4)$$

Now a polyion in a particular orientation that is translating with constant velocity can be viewed as a superposition of T1 and T2 cases with a net force of zero. Solving for $\mathbf{u}$ yields

$$\mathbf{u} = \mathbf{M}\cdot\mathbf{e} \quad (5)$$

$$\mathbf{M} = \mathbf{K}^{-1}\cdot\mathbf{Q} \quad (6)$$

where $\mathbf{M}$ is the electrophoretic mobility tensor. Averaging over all possible orientations leads to the low-field electrophoretic mobility, μ

$$\mu = \frac{1}{3}\mathrm{Tr}(\mathbf{M}) \quad (7)$$

where Tr denotes trace. In summary, determination of $\mathbf{M}$ and μ requires knowledge of the electrostatic potential and ion densities for T1 and T2 transport cases.

Poisson Equation

Both the ion transport and Poisson equations can be cast into forms that are amenable to the boundary element (BE) method. Consider first the Poisson equation

$$\nabla\cdot(\epsilon(\mathbf{x})\nabla\Lambda(\mathbf{x})) = -4\pi\rho(\mathbf{x}) \quad (8)$$

$$\rho(\mathbf{x}) = q\lambda\sum_\alpha z_\alpha n_\alpha(\mathbf{x}) + \rho_f(\mathbf{x}) \quad (9)$$

where Λ is the electrostatic potential, ϵ is the spatially varying dielectric constant, ρ is the net charge density, ρ_f is the fixed charge density associated with the polyion, λ is a screening function equal to zero inside the polyion and one in the fluid, z_α is the valence of mobile ion species α, and $n_\alpha(\mathbf{x})$ is its local concentration at $\mathbf{x}$. If we assume the dielectric constant is ϵ_i/ϵ_o inside/outside the polyion and that there is no surface charge on the polyion surface, S, then

$$\epsilon_i\left(\frac{\partial\Lambda}{\partial n}\right)_{\text{inside}} = \epsilon_o\left(\frac{\partial\Lambda}{\partial n}\right)_{\text{outside}} \quad (10)$$

where the derivatives are outward normal derivatives taken in the limit of a field point approaching S from the interior or exterior of the polyion.

In this work, we shall be interested in the potential in the vicinity of a polyion placed in constant external electric field, $\mathbf{e}$, or translating with constant velocity, $\mathbf{u}$. It is convenient to define a perturbation potential, ψ, through

$$\Lambda = \Lambda_0 + \psi - \mathbf{e}\cdot\mathbf{r} \quad (11)$$

where Λ_0 is the potential of a stationary polyion in the absence of an external electric or flow field. Far from the polyion, $\Lambda_0 \approx 0$, $\Lambda \approx -\mathbf{e}\cdot\mathbf{r}$, so $\psi \approx 0$. We shall also introduce the additional potentials, Φ_α, which represent the departure of n_α from its equilibrium value, $n_{\alpha o}$, as done by O'Brien and White[15]

$$n_\alpha(x) = n_{\alpha o}(x)e^{-\beta z_\alpha q(\psi(x)+\Phi_\alpha(x))} \simeq n_{\alpha o}(x)[1 - \beta z_\alpha q(\psi(x) + \Phi_\alpha(x))] \quad (12)$$

$$n_{\alpha o}(\mathbf{x}) = c_{\alpha o}e^{-\beta z_\alpha q\Lambda_0(\mathbf{x})} \quad (13)$$

where $\beta = 1/k_B T$ and $c_{\alpha o}$ is the ambient concentration of ion α. The assumption will be made that the departure of n_α from its equilibrium value is small. Hence, the exponential in eq 12 is expanded and only the leading term retained. This will account for effects that are linear in the applied field strengths. Both Λ_0 and ψ are obtained by solving Poisson's equation, and Φ_α is obtained by solving the ion transport equation which is discussed later. It will prove convenient to solve for Λ_0 and ψ separately. Consider first the solution of Λ_0. The charge distribution inside the polyion is assumed to consist of an arbitrary distribution of point charges of valence z_p and position $\mathbf{x}_p$. Equations 8 and 9 become

$$\nabla^2\Lambda_0(\mathbf{x}) = h_0'(\mathbf{x}) \quad (14)$$

$$h_0'(\mathbf{x}) = -\frac{4\pi q}{\epsilon_i}\sum_p z_p \delta(\mathbf{x} - \mathbf{x}_p) \qquad \mathbf{x} \in V_i \tag{15}$$

$$= -\frac{4\pi q}{\epsilon_o}\sum_\alpha z_\alpha n_{\alpha o}(\mathbf{x}) \qquad \mathbf{x} \in V \tag{16}$$

where δ is the delta function, V_i represents the polyion interior, and V is the solvent domain. The ion densities, $n_{\alpha o}$, are given by eq 13, and it should be emphasized that this is not linearized. Equation 10 provides the boundary condition

$$g_0(\mathbf{x}) = \epsilon_i\left(\frac{\partial \Lambda_0(\mathbf{x})}{\partial n}\right)_{\text{inside}} = \epsilon_o\left(\frac{\partial \Lambda_0(\mathbf{x})}{\partial n}\right)_{\text{outside}} \tag{17}$$

In this work $\Lambda_0(\mathbf{x})$ is solved by a procedure similar to that used by Zhou[22] which extends the BE method applied to the linear Poisson−Boltzmann equation[23−25] to the nonlinear case. The details of the BE approach are described in the Appendix. The first step is to compute Λ_0 and g_0 on the polyion surface. As described in previous work,[17] the polyion surface is broken into a series of N flat triangular platelets and the assumption is made that Λ_0 and g_0 are constant over each platelet. Equations A26 and A27 are used to solve for the N Λ_0's and g_0's. (Λ_{0j}, g_{0k}/ϵ_o, and g_{0k}/ϵ_i replace ψ_j, p_k^e, and p_k^i in eqs A26 and A27.) For the parameter α, the Debye−Huckel screening parameter, κ, is used where

$$\kappa^2 = \frac{4\pi q^2}{\epsilon_o k_B T}\sum_\alpha c_{\alpha 0} z_\alpha{}^2 \tag{18}$$

The advantage of making this choice is that the external source term, v_j^e in eq A27, vanishes everywhere in the solvent domain except where nonlinear terms in eq 13 are significant. The external source terms do pose a problem since they contain Λ_0, which is what we are trying to determine. Consequently, an iterative approach is followed in which successive estimates of Λ_0 are used in the source terms. In the first iteration, the v_j^e's are set to zero and the first estimates of Λ_{0j} and g_{0j} are obtained by solving eqs A26 and A27. In this work, eqs A26 and A27 are put in the form of a $2N \times 2N$ matrix product. A $2N \times 2N$ matrix is computed and inverted once at the start of the calculation and saved for subsequent iterations. The first estimates of Λ_{0j} and g_{0j} represent solutions of the linearized Poisson−Boltzmann equation. Then, eq A28 is used to compute $\Lambda_0(\mathbf{s})$ in the exterior domain which is discretized into M volume elements. In this work the exterior domain is divided into J (typically 50−100) shells or "onion skins" that conform closely to the polyion surface. Each shell, in turn, is subdivided into N five-sided volume elements (truncated pyramids). For the innermost shell, one side of the volume element corresponds to one of the N polyion surface platelets. Once Λ_0 is computed at the centroid of each of the volume elements, the v_j^e's can be computed using eqs A7, A13, A17, and A29, and these represent the source terms for the second iteration. The procedure of first computing new surface Λ_{0j} and g_{0j}, then using these to compute updated $\Lambda_0^{(j+1)}(\mathbf{s})$ (where $j + 1$ represents the new iteration), and finally using these to compute new v_j^e can be repeated until the potentials converge. We have found it necessary to modify this approach in one respect due to divergence of the potentials in certain cases. The updated potentials, $\Lambda_0^{(j+1)}$, are computed as discussed above, but the previous estimate, $\Lambda_0^{(j)}$, is retained in memory ($j = 1$, 2, etc.). Rather than using $\Lambda_0^{(j+1)}$ to compute the new v_j^e, a scaled potential is used instead

$$\Lambda_0^* = \Lambda_0^{(j)} + \lambda(\Lambda_0^{(j+1)} - \Lambda_0^{(j)}) \tag{19}$$

For a single central charge of +66.572 placed at the center of a 2 nm sphere and a monovalent salt concentration of 0.576 M, no scaling is necessary ($\lambda = 1$). The surface potential in this case is $3k_BT/q$ which is large enough for ion relaxation to be important. However, for charge distributions involving displaced single charges of comparable size or dipolar or quadrupolar charge distributions, scaling was necessary (typically $\lambda \approx 0.25$).

The procedure for determining ψ is very similar. Equations 8 and 9 are replaced with

$$\nabla^2\psi(\mathbf{x}) = h'(\mathbf{x}) \tag{20}$$

$$h'(\mathbf{x}) = 0 \qquad \mathbf{x} \in V_i \tag{21}$$

$$h'(\mathbf{x}) = \frac{4\pi q^2}{\epsilon_o k_B T}\sum_\alpha n_{\alpha 0}(\mathbf{x}) z_\alpha{}^2(\psi(\mathbf{x}) + \Phi_\alpha(\mathbf{x})) \qquad \mathbf{x} \in V \tag{22}$$

The boundary conditions on the polyion surface are a little different due to the possible presence of the external field, **e**

$$\epsilon_i\left(\frac{\partial \psi(\mathbf{x})}{\partial n}\right)_{\text{inside}} = g(\mathbf{x}) - (\epsilon_o - \epsilon_i)\mathbf{e}\cdot\mathbf{n}(\mathbf{x}) \tag{23}$$

$$g(\mathbf{x}) = \epsilon_o\left(\frac{\partial \psi(\mathbf{x})}{\partial n}\right)_{\text{outside}} \tag{24}$$

where $\mathbf{n}(\mathbf{x})$ is a local outward normal from the polyion surface at $\mathbf{x}$. With minor modifications, the procedure used to compute Λ_0 can be used to compute ψ. At the beginning of the calculation, ion relaxation is ignored so $\psi = -\Phi_\alpha$ (see eq 12) and eq 22 above equals 0. Setting $\alpha = 0$ in eq A26, eqs A26 and A27 can be solved to obtain a first estimate of ψ. Physically, $(\psi - \mathbf{e}\cdot\mathbf{r})$ is the potential of the uncharged, low dielectric polyion placed in constant external field, **e**. Before a new estimate of ψ is made, new estimates of the Φ_α are determined as described later. These along with (scaled) ψ's are then used to determine v_j^e. Also, the term $(\epsilon_o - \epsilon_i)(\mathbf{e}\cdot\mathbf{n})$ appearing in eq 23 is absorbed into v_j^i. Then, eqs A26 and A27 are used to determine ψ_j and g_j followed by the use of eqs A28 or A33 and A30 or A36 to determine ψ and $\nabla\psi$ in the exterior domain. As in the case of Λ_0, the new $\psi^{(j+1)}$ is replaced with $\psi^{(j)} + \lambda(\psi^{(j+1)} - \psi^{(j)})$ before computing the new v_j^e. To summarize, updating the ψ's is done in tandem with the Φ_α's but the procedure is otherwise similar to the iterative procedure used for Λ_0. Our attention shall now be turned toward the determination of Φ_α.

Ion Transport Equation

In order to obtain Φ_α, the ion transport equation must be solved. The calculation is carried out in a reference frame stationary with respect to the polyion and steady state conditions are assumed to prevail. The equation of continuity yields

$$0 = \nabla\cdot\mathbf{j}_\alpha(\mathbf{x}) \tag{25}$$

where $\mathbf{j}_\alpha$ is the local current density of ion α. It is given by

$$\mathbf{j}_\alpha = n_\alpha \mathbf{v} - D_\alpha \nabla n_\alpha + \beta n_\alpha D_\alpha \mathbf{s}_\alpha \tag{26}$$

where $\mathbf{v}$ is the local fluid velocity, D_α is the diffusion constant of ion α, and $\mathbf{s}_\alpha$ is the local force on ion α which is taken to be

$$\mathbf{s}_\alpha = -z_\alpha q(\nabla\Lambda_0 + \nabla\psi - \mathbf{e}) \tag{27}$$

Making use of eqs 12 and 13 and retaining terms to first order in the external electric or flow field lead to

$$\mathbf{j}_\alpha = n_{\alpha 0}\mathbf{v} + \beta D_\alpha z_\alpha q n_{\alpha 0}(\nabla\Phi_\alpha + \mathbf{e}) \tag{28}$$

Substituting this into eq 25 and assuming solvent incompressibility ($\nabla\cdot\mathbf{v} = 0$) gives

$$\nabla^2\Phi_\alpha = f_\alpha \tag{29}$$

$$f_\alpha = \left[\frac{1}{D_\alpha}\mathbf{v} + \beta z_\alpha q(\nabla\Phi_\alpha + \mathbf{e})\right]\cdot\nabla\Lambda_0 \tag{30}$$

where the above two equations are restricted to the solvent domain. As in the case of the Poisson equation, there is a boundary condition at the polyion surface (where $\mathbf{v} = 0$ due to our choice of reference frame) which arises from the impermeability of the polyion to the passage of ions: $\mathbf{j}_\alpha\cdot\mathbf{n} = 0$. From eq 28 this requires

$$\left(\frac{\partial\Phi_\alpha(\mathbf{x})}{\partial n}\right)_{\text{outside}} = -\mathbf{e}\cdot\mathbf{n}(\mathbf{x}) \tag{31}$$

As in the case of the solution of Λ_0 and ψ, the boundary element approach is used to solve for Φ_α. Since $\nabla\Phi_\alpha$ appears in the source term, f_α (eq 30), it is also necessary to use an iterative approach in which previous estimates of Φ_α are used to update f_α, which are then used to update Φ_α. The source term also contains $\nabla\Lambda_0$ (computed previously and saved at discrete points in the solvent domain) and the local fluid velocity, $\mathbf{v}$. The local fluid velocity is also updated after each iteration and its calculation is described in the next section.

As an initial estimate, ion relaxation is ignored and we simply set $\Phi_\alpha = -\psi$ (eq 12) where ψ has been computed previously. Also, initial fluid velocities are computed (assuming no ion relaxation) and eq 30 is used to compute initial f_α's. Prior to solving eq A26 to obtain the surface Φ_α's, the v_j^e's must be computed (f_α replaces h' in eqs A7 and A29). Also, the p_k^e's are given by eq 31. For the α parameter appearing in eq A26, we simply set it to 0. It has been our experience that the most efficient choice of α is the one which minimizes h (eq A7) in the solvent domain. Due to the presence of the $\nabla\Lambda_0$ term in f_α, f_α falls off quickly with distance from the polyion surface and setting $\alpha = 0$ ensures that h is small in most of the solvent domain. Once the surface Φ_α's are computed, eqs A28 or A33 is used to determine Φ_α and eqs A30 or A34−A36 to determine $\nabla\Phi_\alpha$ in the solvent domain. These along with recomputed $\mathbf{v}$'s (next section) allow us to recompute the source terms for subsequent iteration.

In addition, we would like to discuss an approach which has been found to yield a better estimate of the normal component of $\nabla\Phi_\alpha$ near the polyion surface. Equation 25 is integrated over a particular volume element (solvent domain), and application of the divergence theorem results in a surface integral. This surface integration involves three "tangential" surfaces and two "normal" surfaces given the way we have discretized the solvent domain. The inner "normal" derivative of Φ_α is known either from the surface boundary condition, eq 31 (at the polyion surface), or from a previous calculation over an inner shell of volume elements. Also, the three tangential derivatives of Φ_α (appearing in the integration of eq 28 over the tangential surfaces) are computed according to eqs A34−A36. Since the net flux of $\mathbf{j}_\alpha$ through the five surfaces must vanish, we can estimate the normal derivative of Φ_α at the outer "normal" surface. This is basically the strategy employed by O'Brien[7] and Anderson and co-workers[8] in related work on thin double layers. Here, this approach is used to calculate the normal derivatives for the innermost (typically 4) shells of volume elements.

Calculation of Fluid Velocities

The fluid velocity calculation involves numerical solution of the Navier−Stokes equation which has been described in detail previously,[17,20,26] so only a brief review is given here. As in the case of the Poisson and ion transport equations, a BE method is employed which utilizes the singular solution of the Navier−Stokes equation. Given a rigid polyion translating with velocity $\mathbf{u}$ through an incompressible fluid which is at rest far from the polyion, the fluid velocity at $\mathbf{r}$ is given by

$$\mathbf{v}(\mathbf{r}) = -\int_S \mathbf{U}(\mathbf{x},\mathbf{r})\cdot\mathbf{w}(\mathbf{x})\,dS_x - \int_V \mathbf{U}(\mathbf{x},\mathbf{r})\cdot\mathbf{s}(\mathbf{x})\,dV_x \tag{32}$$

where S, V, and $\mathbf{s}$ have the same meaning as before and $\mathbf{w}$ represents the surface stress force per unit area. (The total hydrodynamic force is obtained by integrating $\mathbf{w}$ over the entire polyion surface.) $\mathbf{U}$ is given by

$$\mathbf{U}(\mathbf{x},\mathbf{r}) = -\frac{1}{8\pi\eta y}[\mathbf{I} + \mathbf{R}(\mathbf{x},\mathbf{r})] \qquad (\mathbf{R}(\mathbf{x},\mathbf{r}))_{ij} = \mathbf{y}_i\mathbf{y}_j/y^2 \tag{33}$$

where η is the fluid viscosity, $\mathbf{y} = \mathbf{r} - \mathbf{x}$, $y = |\mathbf{y}|$, and $\mathbf{I}$ is the 3×3 identity matrix. As discussed previously, the surface is discretized into N platelets and the surrounding fluid into M volume elements. The assumption is made that $\mathbf{w}/\mathbf{s}$ is constant over each surface/volume element. Equation 32 can be written

$$\mathbf{v}(\mathbf{r}) = \sum_{j=1}^{N}\mathbf{E}_j(\mathbf{y})\cdot\mathbf{w}_j + \sum_{k=1}^{M}\mathbf{G}_k(\mathbf{y})\cdot\mathbf{s}_k \tag{34}$$

where $\mathbf{E}_j/\mathbf{G}_k$ are surface/volume integrals over $\mathbf{U}$. At the polyion surface, stick boundary conditions are assumed which requires $\mathbf{v} = \mathbf{u}$ at the polyion surface. The only unknowns in eq 34 are the $\mathbf{w}_j$'s which can be readily computed by inverting a $3N \times 3N$ matrix.

Rather than using actual external forces ($\mathbf{s} = -\rho\nabla\Lambda$) in eqs 32 and 34, O'Brien and White[15] have shown that the same velocity field is obtained using fictitious force, $\mathbf{s}'$, defined by

$$\mathbf{s}' = \sum_\alpha n_{\alpha 0} z_\alpha q(\nabla\Phi_\alpha + \mathbf{e}) \tag{35}$$

provided the same boundary condition on $\mathbf{v}$ is employed. The advantage of this approach is that $\mathbf{s}'$ and consequently $\mathbf{v}$ is independent of the perturbation potential, ψ. The connection between $\mathbf{s}'$ and $\mathbf{s}$ is

$$\mathbf{s} = \mathbf{s}' + \nabla\pi \tag{36}$$

$$\pi = k_B T \sum_\alpha n_\alpha \tag{37}$$

where π is the osmotic pressure within an additive constant.

Results

In the Appendix, special procedures are described for treating potentials and potential gradients near the polyion surface. An uncharged low dielectric sphere placed in a constant external electric field, **e**, provides a good illustration of the BE approach. The sphere radius is taken to be $a = 2$ nm and ϵ_i/ϵ_o is taken to be 2/78. The sphere is represented as a 128 (or 512) platelet geodesic surface and the electric field is 1 kV/cm directed along the $-x$-axis. The procedure used to generate the surface is briefly described later. The analytical form of $\psi(\mathbf{s})$ (the actual potential plus $\mathbf{e}\cdot\mathbf{s}$ according to eq 11) is given by

$$\psi(\mathbf{s}) = -\left(\frac{\epsilon_o - \epsilon_i}{2\epsilon_o + \epsilon_i}\right)\left(\frac{a}{s}\right)^3 (\mathbf{s}\cdot\mathbf{e}) \tag{38}$$

in the external solvent domain. The root-mean-square (rms) surface potential is expected to be 1.849×10^{-7} erg/esu from eq 38 compared to 1.899×10^{-7} erg/esu derived from solution of the BE problem (eqs A26 and A27) with $\alpha = 0$ and $N = 128$. Also, the rms g (see eq 24) is expected to be 1.443×10^{-5} erg/(esu nm) compared to 1.442×10^{-5} obtained from BE. The surface potential and g are in error by 4% and 0.3%, respectively ($N = 128$). The centroids of all volume elements within a particular shell are about the same distance from the center of the polyion. Shown in Figure 1 are rms ψ's (obtained by averaging all potentials within a given shell) versus distance ($N = 128$). The top curve represents the numerical solution of eq A28 for exterior points. For corresponding mirror points inside the polyion, the right hand side (rhs) of eq A32 should vanish in principle but may not in practice due to discretization and numerical error. However, Figure 1 does show that the rhs of eq A32 is close to zero. What this means is that the mirror point correction procedure (eq A33) does not significantly improve ψ near the polyion surface in this particular example. However, a quite different conclusion is reached when the gradient of ψ is considered. First of all define

$$\mathrm{GT} = \langle(\nabla\psi - \mathbf{n}(\mathbf{n}\cdot\nabla\psi))^2\rangle^{1/2} \tag{39}$$

$$\mathrm{GN} = \langle(\mathbf{n}\cdot\nabla\psi)^2\rangle^{1/2} \tag{40}$$

where brackets denote an average over all volume elements within a particular shell and **n** is the local outward unit normal to the polyion surface. The tangential gradient component, GT, is plotted in Figure 2 for $N = 128$. Without any mirror correction (eq A30), the BE procedure does not yield accurate tangential gradients near the polyion surface. However, better results are obtained when eq A34 is used which corresponds to adding the gradient of ψ at the field and mirror points. Still better results are obtained by going to a surface made up of 512 platelets, as shown in Figure 3. For $N = 128$, the normal gradient component is computed more accurately in this particular example than the tangential gradient, as shown in Figure 4. As discussed in the Appendix, we expect that subtracting the gradients (eq A35) should improve the accuracy in this case and the results of Figure 4 are consistent with this. Unless otherwise stated, eq A36 is used for all field points within a 0.3 nm distance of the polyion surface. This ensures that the sum formula is used for the tangential and difference formula is used for the normal gradient components.

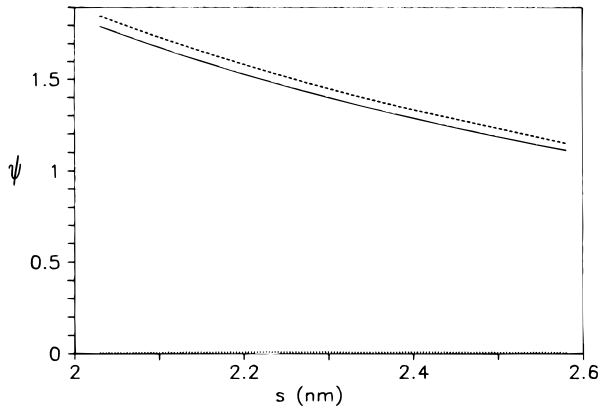

Figure 1. ψ versus s for an uncharged sphere in an electric field. The solid line is the analytic ψ from eq 38, and the BE result for $N = 128$ is the dashed line. The mirror image correction (from the rhs of eq A32) is the dotted line.

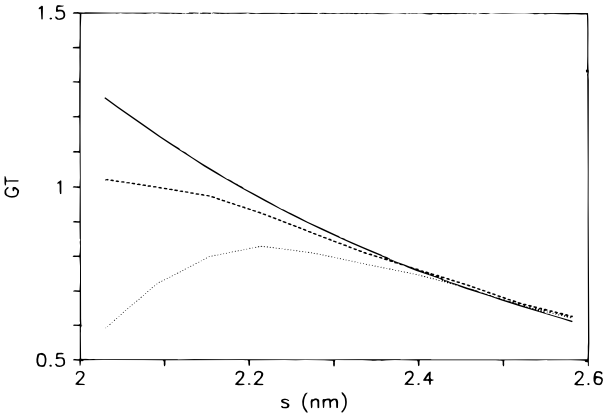

Figure 2. GT versus s for an uncharged sphere in an electric field. The solid line is the analytic curve, the dotted line is the uncorrected BE curve (from eq A30), and the dashed line is the corrected BE curve (from eq A34). In the BE calculations, $N = 128$.

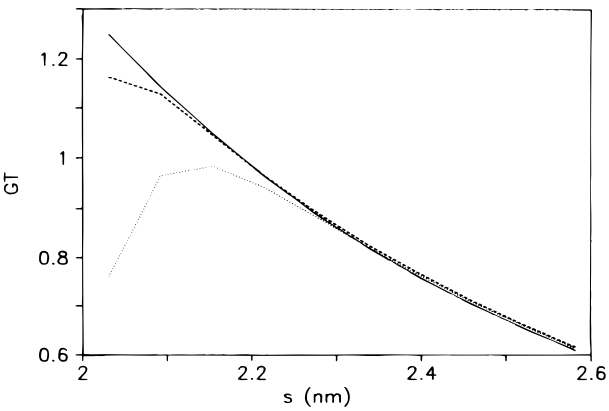

Figure 3. GT versus s for an uncharged sphere in an electric field. Same as Figure 2, but $N = 512$.

Attention shall now be turned to simple models of highly charged polyions with salt present. Consider a spherical polyion containing a single charge located at its center. A polyion radius of 2 nm is chosen immersed in a monovalent salt of ambient concentration 0.576 M. The interior/exterior dielectric constants are taken to

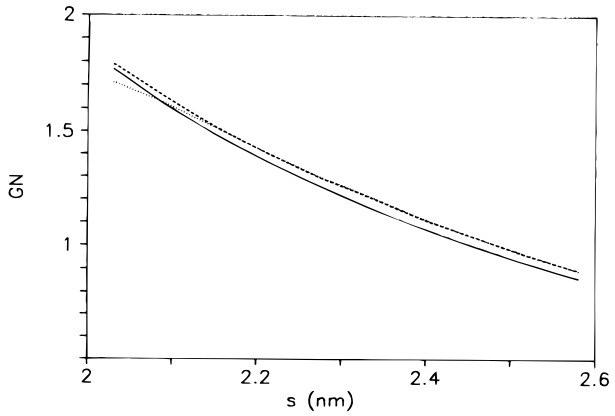

Figure 4. GN versus *s* for an uncharged sphere in an electric field. Similar to Figure 2 except for the normal component ($N = 128$). The solid curve is the analytic value, and the dotted line is the uncorrected BE result (from eq A30). The dashed curved comes from eq A35.

be 2/78, and the temperature and solvent viscosity are set to 25 °C and 0.0089 P, respectively. This gives $\kappa a = 5$. For the co-ions and counterions, an effective hydrodynamic radius of 0.132 nm shall be used which gives $m_\alpha = 0.184$ ($\alpha = \pm 1$) where

$$m_\alpha = \frac{\epsilon_o k_B T f_\alpha}{6\pi\eta q^2} \tag{41}$$

and $f_\alpha = k_B T/D_\alpha = 6\pi\eta a_\alpha$ is the friction coefficient of ion α. This value of m_α was used extensively by Wiersema et al.[13,14] and is typical for monovalent ions. A central charge of $+66.572q$ is used which yields a reduced potential

$$y_0(r) = \beta q \Lambda_0(r) \tag{42}$$

of about 3 at the polyion surface under these conditions.[20] A surface potential of this magnitude is large enough to ensure that ion relaxation is significant.[13,14,20] In addition, this case was extensively studied in previous work[20] and we can check not only y_0 and mobilities but also Φ_α's.

As in previous modeling studies of rigid polyions[17] the tesselation procedure of Pakdel and Kim[27] is used to represent the sphere as a geodesic surface of $N = 128$ or 512 triangular platelets. There are also N/2 + 2 vertex vectors of equal length associated with each geodesic surface and a given vertex vector represents the corner of 4 or 6 different platelets. To determine the appropriate size of the vertex vectors, several T1 calculations are carried out for uncharged model polyions and that vertex vector length which gives a translational friction constant ($6\pi\eta a$) appropriate for a 2 nm sphere is determined by interpolation.

Consider the reduced polyion potential, y_0, given by eq 42. The BE method is used to solve the nonlinear PB equation following the procedure described previously. Twelve iterations have been carried out, and the volume around the polyion is subdivided into 50 shells each consisting of N truncated pyramids of thickness 0.0306 nm. The results are summarized in Table 1. Averages over all quantities in the same shell are denoted by brackets, $\langle\rangle$, and s represents the distance of the centroid of a particular volume element from the polyion center. The "exact" reduced potential, y_{Loeb}, is solved for by numerically following the algorithm of Loeb et al.,[28] and y_0 represents BE results. The error

Table 1. Comparison of Exact (y_{Loeb}) and BE-Reduced Potentials

		$N = 128$		$N = 512$	
$\langle s \rangle$	$\langle y_{Loeb} \rangle$	$\langle y \rangle$	error	$\langle y \rangle$	error
2.03	2.67	2.74	0.082	2.71	0.042
2.09	2.14	2.21	0.071	2.18	0.037
2.15	1.75	1.80	0.055	1.77	0.027
2.21	1.44	1.47	0.038	1.45	0.021
2.27	1.19	1.21	0.027	1.20	0.017
3.01	0.14	0.142	0.005	0.140	0.001
4.05	0.00773	0.0079	0.00011	0.00768	0.0002
5.03	0.000538	0.000542	0.000006	0.000535	0.000002

Table 2. Total Polyion Forces (in 10^{-8} Dyne) Versus Iteration Number

	$N = 128$		$N = 512$	
iteration	T1	T2	T1	T2
0	3.355	−1.629	3.355	−1.598
1	3.429	−1.286	3.449	−1.184
2	3.415	−1.235	3.426	−1.175
3	3.409	−1.314	3.419	−1.262
4	3.406	−1.337	3.417	−1.286
5	3.405	−1.340	3.415	−1.29
6	3.404	−1.342	3.415	
7		−1.341		

represents $\langle (y_0 - y_{Loeb})^2 \rangle^{1/2}$ where again the average is taken over all volume elements within a particular shell. Near the polyion surface, the relative error is about 3% for $N = 128$ and about 1.5% for $N = 512$.

The efficacy of the BE procedure in yielding electrostatic potentials around model polyions was well-known before we undertook this project. Of paramount concern to us was whether or not the resulting potentials are accurate enough to yield meaningful electrophoretic mobilities. To answer this question, the results of detailed T1 and T2 calculations shall be described for the 2 nm sphere containing a central charge of $+66.572q$. Other parameters are the same as those discussed previously ($y_0(a) \approx 3$). Briefly, the calculation begins by reading in information about the polyion surface and charge distribution as well as Λ_0 in the solvent domain. As a first approximation, ion relaxation is ignored and eq 1 is used to compute the total force on the polyion in T1 and T2 transport cases.[17] Then the calculation enters an iterative cycle in which first $\mathbf{v}$, and then Φ_α and ψ and their gradients are computed by BE procedures. This is the most time consuming part of the calculation. Once these are known, the forces $\mathbf{s}$ (eq 2) and $\mathbf{s}'$ (eq 35) are computed followed by reapplication of eq 1 to update the total force on the polyion. The iterative cycle is repeated until the forces converge. Summarized in Table 2 are total forces versus iteration number for T1 and T2 transport cases for $N = 128$ and 512. In the T1 calculations, the polyion is translated with velocity 1 cm/s in the $-x$ direction, and in the T2 calculations, the stationary polyion is placed in an electric field of magnitude 1 kV/cm directed along $-x$. From eqs 3−7 we can express the mobility for this case

$$M_{ii} = -\frac{z_i(2)u_i(1)}{z_i(1)e_i(2)} \tag{43}$$

and the reduced mobility is defined

$$\gamma_{ii} = \frac{6\pi\eta q M_{ii}}{\epsilon_o k_B T} \tag{44}$$

For the sphere containing a central charge, γ will be

isotropic. In the absence of relaxation, γ should equal 3.41[13,14] and the BE calculations (from iteration no. 0 results of Table 2) yield 3.66 (high by 7.3%) and 3.56 (high by 5.2%) for $N = 128$ and 512, respectively. Including ion relaxation, γ should be 2.74[13,14] and the BE calculations yield 2.97 (high by 9.1%) and 2.85 (high by 3.8%) for $N = 128$ and 512, respectively. These results show that for this test case, the BE procedure is yielding mobilities accurate to within 10% even for the low-resolution model consisting of $N = 128$ platelets. Increasing N by a factor of 4 yields more accurate mobilities, which is to be expected.

In addition to the mobilities, it is possible to compare Φ_α obtained by the present BE procedure with a closely related quantity, g_α, determined previously by somewhat different methods.[20] The two quantities are related by

$$\Phi_\alpha = \frac{k_B T}{q} g_\alpha \cos\theta \tag{45}$$

where g_α depends only on s and θ is the angle between **s** and the flow field/electric field direction. For the T2 case considered in ref 20 $\langle(\Phi_{+1}(a))^2\rangle^{1/2} = 2.84 \times 10^{-7}$ erg/esu and $\langle(\Phi_{-1}(a))^2\rangle^{1/2} = 0.77 \times 10^{-7}$ erg/esu, where brackets denote an average over the spherical surface. For $N = 128$, the variation of $\langle(\Phi_{+1}(a)^2\rangle^{1/2}$ (in 10^{-7} erg/esu) with iteration number is 3.51, 2.55, 3.06, 2.98, 2.93, 2.96, and 2.95. The corresponding variation in $\langle(\Phi_{-1}(a)^2\rangle^{1/2}$ is 0.38, 0.93, 0.90, 0.75, 0.72, 0.72, and 0.74. Thus, there is good agreement between the two independent calculations which leads us to conclude that ion relaxation is being properly accounted for. Increasing N to 512 has little effect on Φ_α.

Before leaving the transport of a sphere with a centrosymmetric charge distribution, we would like to consider the effect of the velocity field, **v**, on the T2 transport case (where the polyion is held stationary in a solvent which is also stationary far from the polyion). Net charge densities near the polyion surface can be significant, and the presence of external electric fields exerts forces on the fluid which, in turn, produce fluid convection. These convective effects are known to be important, for example, in the alignment of long, charged rodlike molecules in electric fields,[29] and we would like to assess their importance in the electrophoresis of spherical polyions. From Table 2, it is clear that ion relaxation has a significant effect on T2 but not T1 transport cases. Convection enters the problem explicitly through the **v** term appearing in the ion transport equation (eqs 28 and 30). If convection is important, then leaving it out of the calculation should have a significant effect on the total polyion force. Leaving it out (T2, $N = 128$) changes the total force from -1.341×10^{-8} to -1.383×10^{-8} dyne so the effect is seen to be small in this particular example.

Attention shall now be turned to some other charge distributions. In the following examples, the polyion shape is spherical with parameters identical to those used previously for the centrosymmetric charge distribution. The charges are placed along the x-axis and $N = 128$ except for one of the quadrupole cases considered. In case a, a charge $Q = +66.572q$ is placed at (0.5, 0, 0). This is similar to the centrosymmetric example considered previously except the charge is displaced from the origin by 0.5 nm. The reduced mobilities are given in Table 3 (first entry). Because of the placement of the charge, the mobility is expected to be different along the axis which passes through the center of friction (origin of the sphere in this case) and the charge (the x-axis) and a perpendicular direction (z-axis). At low field strengths, the reduced mobility should be given by

$$\gamma = \frac{1}{3}(\gamma_{xx} + 2\gamma_{zz}) \tag{46}$$

which for the displaced monopole turns out to be 3.65 (no relaxation) and 2.85 (relaxation). These are so similar to those of the centrosymmetric charge distribution that we conclude they are indistinguishable at the level of accuracy of these calculations.

Table 3. Reduced Mobilities of Spherical Polyions With Noncentrosymmetric Charge Distributions (Charge Distributed along *x*-Axis)

	no relax		relax	
case	γ_{xx}	γ_{zz}	γ_{xx}	γ_{zz}
a. displaced monopole	3.56	3.69	2.75	2.90
b. dipole	(0)	(0)	(0)	(0)
c. quadrupole, $N = 128$	0.901	−0.152	0.859	−0.133
d. quadrupole, $N = 512$	0.793	−0.152	0.839	−0.152

In case b, a dipole with $\pm Q = \pm 66.572q$ is placed at ($\pm$0.5, 0, 0). This model polyion has no net charge, and the even moments of its charge distribution are negligible. The mobility (second entry of Table 3) is calculated to be negligible. Yoon[30] has developed an analytical theory of electrophoresis of spherical polyions containing an arbitrary charge distribution. However, ion relaxation is ignored in this theory and the additional assumption is made that the ion atmosphere is distributed according to the linearized Poisson−Boltzmann equation. The main conclusions of the Yoon theory relevant to the present work are (i) only the monopole and quadrupole moments of the charge distribution contribute to the mobility and (ii) the contribution of the quadrupole vanishes when an isotropic average is taken over all possible orientations. Thin double layer theories (in which the surface potentials can be arbitrarily large) have also considered the dependence of electrophoretic mobility on charge distribution. In the absence of relaxation, only the monopole and quadrupole moments contribute but, unlike the Yoon theory, the contribution of the quadrupole does not necessarily vanish upon averaging over all possible orientations.[6] With relaxation, other moments appear to contribute with the exception of the dipole moment.[8] It should be emphasized, however, that the dipole will contribute at high field strength, since it serves to orient the polyion to some degree, and taking an isotropic average over all orientations is no longer valid. In any event, both the displaced monopole and dipole results obtained in this work are qualitatively consistent with the Yoon[30] and thin double layer[6,8] theories.

The last two entries in Table 3 correspond to a quadrupole distribution in which a charge of $+66.76q$ is placed at the origin and $-33.38q$ is placed at ($\pm$1, 0, 0). The total charge is 0. Ion relaxation has a smaller effect than in the monopolar cases considered previously. From eq 46 and Table 3, the reduced mobility for $N = 128$ is 0.199 (no relaxation) and 0.198 (relaxation) and for $N = 512$ is 0.165 (no relaxation) and 0.178 (relaxation). At variance with the Yoon theory but not thin double layer theories, the mobility of this quadrupolar polyion does not vanish.

To conclude, we would like to compare the mobilities obtained here with the reduced mobility, γ_{tdl}, predicted by thin double layer theory in the absence of relaxation[6]

$$\gamma_{tdl} = \frac{3}{2}\beta q\langle\Lambda_0\rangle \tag{47}$$

where the average is taken over the polyion surface. It is convenient to characterize the surface potential of a spherical polyion by expanding it in terms of Legendre Polynomials, P_j,

$$\beta q\Lambda_0(\mathbf{s}) = \sum_j c_j P_j(\cos\theta) \tag{48}$$

where **s** is some point on the polyion surface and $\cos\theta = n_x$ where n_x is the x component of the local surface outward normal. The coefficients, c_j, are readily obtained from averages over the surface of the polyion

$$c_j = (2j+1)\beta q\langle\Lambda_0(\mathbf{s})P_j(n_x)\rangle \tag{49}$$

The c coefficients are summarized in Table 4 for the four cases included in Table 3. Also included are the centrosymmetric monopole, $N = 128$ (case e) and $N = 512$ (case f). As expected, the overwhelming component of cases e and f is c_0, case b is c_1, and cases c and d is c_2. The displaced monopole, on the other hand, has significant contributions from c_0 through c_2. It is also evident from this table that γ_{tdl} exceeds the actual mobility by about 40%, which is attributed to the thickness of the double layer. For the polyions considered in this work, the double layer thickness must be accounted for.

Table 4. Reduced Potential Coefficients and γ's

case	c_0	c_1	c_2	c_3	γ_{tdl}	γ(relax)
a	3.26	1.90	0.703	0.159	4.89	2.85
b	0.000	4.76	0.003	−0.637	0	0
c	0.200	−0.012	−3.93	0.023	0.300	0.198
d	0.168	−0.002	−3.79	−0.004	0.252	0.178
e	3.34	0.011	0.009	−0.010	5.01	2.97
f	3.14	0.002	−0.001	0.001	4.71	2.85

Summary

The primary objective of this work is the development of an algorithm to calculate the eletrophoretic mobility of model rigid polyions that accounts for the effect of ion relaxation. It extends previous work which left ion relaxation out.[17] Including ion relaxation complicates the theory substantially because the co-ion and counterion charge distributions and their transport as well as the fluid flow near the polyion are inextricably coupled. This coupling requires simultaneous solution of the Navier−Stokes, Poisson, and ion transport equations. In the present work this is accomplished by solving the three equations using boundary element methods. One starts with the no relaxation limit and iterates the solutions until they converge to a constant value. As a benchmark, the algorithm is first applied to a spherical polyion containing a centrosymmetric charge distribution and a reduced surface potential of about 3. This surface potential is large enough to ensure that ion relaxation makes a significant contribution to the electrophoretic mobility. The resulting mobilities are in good to excellent agreement with the predictions of Wiersema.[13,14] In addition, the distortion of the co-ion and counterion densities at the polyion surface are similar to those obtained previously by a different approach.[20]

The algorithm is then applied to a number of spherical polyions in which the charge distribution is noncentrosymmetric. For a sphere containing a single charge, the ensemble-averaged mobility appears to be fairly insensitive to the position of that charge. A purely dipolar charge distribution has zero mobility, but a quadrupolar charge distribution (net charge of 0) does have a finite value even after averaging over all orientations. However, ion relaxation does not appear to significantly affect the orientationally averaged mobility for the examples studied in the present work. A comparison of the present results with the prediction of thin double layer theory shows the importance of accounting for the double layer thickness when the polyion/particle size is on the order of 2 nm.

Although the models studied in this work were all spherical, there should be no problem in extending these studies to nonspherical models such as ellipsoids or surfaces derived from the space-filling crystal structures of proteins or nucleic acids.[17,19] The objective of the present work was to verify that the algorithm is working (as the results on the sphere with a central charge verify) and then apply it to some simple cases. More complex models will be treated in future studies.

There are aspects of the modeling procedure that could be improved upon in future studies. One of these involves going beyond the Poisson−Boltzmann (PB) equation in calculating Λ_0 more accurately. These could include functional expansion techniques as used by Fixman[31] or Monte Carlo methods used by a number of groups who have been particularly interested in the electrostatic potential of DNA.[32−34] Such refinements are expected to be particularly important if the counterions are multivalent. For univalent salt up to concentrations of several tenths molar, however, these studies have shown that the nonlinear PB equation is quite accurate provided the mobile ion radii are small compared to the polyion radius. A similar conclusion was reached for an electrolyte near a charged wall.[35] Another feature of the problem that has been ignored here is the Brownian motion of the polyion. When a polyion is placed in an electric field, its actual motion will be a superposition of an electrophoretic "drift" and random Brownian displacement. Because Brownian motion causes the polyion position and orientation to change impulsively, we can expect this to influence ion relaxation and hence the electrophoretic mobility. Using a theory by Onsager and co-workers[36] as a starting point, Wiersema[13] studied this problem for a spherical polyion containing a centrosymmetric charge distribution and concluded that the effect is small in that case. For the more complex problem of a noncentrosymmetric charge distribution and/or nonspherical polyion, we might expect the rotational Brownian motion to influence ion relaxation differently. For a spherical polyion containing a dipolar or quadrupolar charge distribution as studied in this work, we can assess the influence of Brownian motion via the following argument. First, Brownian motion has no effect on the low-field, orientationally averaged mobility *in the absence of relaxation*. Second, the present work has shown that ion relaxation has little effect on the mobility of a polyion with a dipolar or quadrupolar charge distribution that is translating under steady state conditions along a particular direction. From this, it follows that Brownian motion should have little effect on the mobility for these cases. Whether or not this is also true for polyions in general is unclear at this time. A final technique which might be able to shed light on this question and which would circumvent the need for boundary element methods altogether is Brownian dynamics simulation where the mobile ions are included explicitly.[37] This approach has the additional advantage of accounting for specific

ion effects and could also be used to study transient phenomena such as the response time of the ion atmosphere to a suddenly imposed electric field. Potential problems might include accounting for the dielectric discontinuity at the polyion−solvent interface, handling long-range electrostatic interations, and carrying out enough Brownian dynamics trajectories of sufficient duration to get accurate mobilities. In conclusion, the present studies could be extended in a number of ways.

Appendix: Boundary Element Method

The starting point of the boundary element (BE) method as applied to the Poisson and ion transport equations is Green's second identity

$$\int_V (F\nabla^2\psi - \psi\nabla^2 F)\,\mathrm{d}V = \int_S (F\nabla\psi - \psi\nabla F)\cdot\mathbf{n}'\,\mathrm{d}S \quad \text{(A1)}$$

where ψ is the potential function we want to determine, F is some trial function, V denotes a volume of integration bounded by some surface(s) S, and $\mathbf{n}'$ is the local unit normal to the surface directed outward from the enclosed volume. We shall use the following trial function

$$F(\alpha,\mathbf{x},\mathbf{s}) = \frac{\mathrm{e}^{-\alpha y}}{4\pi y} \quad \text{(A2)}$$

where $y = |\mathbf{y}| = |\mathbf{x} - \mathbf{s}|$ and

$$\nabla^2 F = \alpha^2 F - \delta(\mathbf{x} - \mathbf{s}) \quad \text{(A3)}$$

In eq A2, α is a constant and the derivative in eq A3 acts on variable $\mathbf{x}$ rather than the field point, $\mathbf{s}$. In this work we are interested in ψ's with the property

$$\nabla^2\psi = h' \quad \text{(A4)}$$

coupled with boundary conditions on the outward unit normal to the polyion surface, $\mathbf{n}$,

$$p = \nabla\psi\cdot\mathbf{n} \quad \text{(A5)}$$

In addition, we shall require $\psi \approx 0$ far from the polyion. The enclosing surface, S, is taken to be the polyion surface. If we choose V to be the polyion exterior and $\mathbf{s}$ to be an exterior point (in the solvent domain), $\mathbf{s}_e$, then eq A1 can be written

$$\psi(\mathbf{s}_e) = -\int_V F(\alpha,\mathbf{x},\mathbf{s}_e)h(\alpha,\mathbf{x})\,\mathrm{d}V_x - \int_S F(\alpha,\mathbf{x},\mathbf{s}_e)p^e(\mathbf{x})\,\mathrm{d}S_x + \int_S F'(\alpha,\mathbf{x},\mathbf{s}_e)\psi(\mathbf{x})\,\mathrm{d}S_x \quad \text{(A6)}$$

where

$$h(\alpha,\mathbf{x}) = h'(\mathbf{x}) - \alpha^2\psi(\mathbf{x}) \quad \text{(A7)}$$

$$F'(\alpha,\mathbf{x},\mathbf{s}) = \nabla_x F(\alpha,\mathbf{x},\mathbf{s})\cdot\mathbf{n} \quad \text{(A8)}$$

and $p^e(\mathbf{x})$ denotes a normal derivative taken from the polyion exterior. (A normal derivative taken from the polyion interior shall be denoted $p^i(\mathbf{x})$.) In this work, α for the exterior problem will either be set to 0 or the Debye−Huckel screening parameter, κ. For the interior problem, α will be set to zero. The analog of eq A6 for a field point in the polyion interior, $\mathbf{s}_i$, is obtained from eq A1 by choosing V to be the polyion interior, V_i.

$$\psi(\mathbf{s}_i) = -\int_{V_i} F(0,\mathbf{x},\mathbf{s}_i)h(0,\mathbf{x})\,\mathrm{d}V_x + \int_S F(0,\mathbf{x},\mathbf{s}_i)p^i(\mathbf{x})\,\mathrm{d}S_x - \int_S F'(0,\mathbf{x},\mathbf{s}_i)\psi(\mathbf{x})\,\mathrm{d}S_x \quad \text{(A9)}$$

There are alternatives to eqs A6 and A9 that are useful in certain cases. If, for example, V is chosen to be the polyion exterior but $\mathbf{s}$ an interior point, then eq A6 is replaced with

$$0 = -\int_V F(\alpha,\mathbf{x},\mathbf{s}_i)h(\alpha,\mathbf{x})\,\mathrm{d}V_x - \int_S F(\alpha,\mathbf{x},\mathbf{s}_i)p^e(\mathbf{x})\,\mathrm{d}S_x + \int_S F'(\alpha,\mathbf{x},\mathbf{s}_i)\psi(\mathbf{x})\,\mathrm{d}S_x \quad \text{(A10)}$$

An analogous relation to eq A9 is obtained if an exterior field point is taken. Now consider an exterior point just outside the polyion surface and move it to the interior. On comparison of eqs A6 and A10, it is seen that the sum of the three integrals on the right hand side must undergo a discontinuous jump as the field point moves across the polyion surface. The first two integrals are continuous, but the third is discontinuous.[23−25] For $\mathbf{s}_i/\mathbf{s}_e$ just inside/outside the polyion surface and $\mathbf{s}_o$ a point on the surface

$$\int_S F'(\alpha,\mathbf{x},\mathbf{s}_e)\psi(\mathbf{x})\,\mathrm{d}S_x = \frac{1}{2}\psi(\mathbf{s}_0) + \int_S F'(\alpha,\mathbf{x},\mathbf{s}_0)\psi(\mathbf{x})\,\mathrm{d}S_x \quad \text{(A11)}$$

$$\int_S F'(\alpha,\mathbf{x},\mathbf{s}_i)\psi(\mathbf{x})\,\mathrm{d}S_x = -\frac{1}{2}\psi(\mathbf{s}_0) + \int_S F'(\alpha,\mathbf{x},\mathbf{s}_0)\psi(\mathbf{x})\,\mathrm{d}S_x \quad \text{(A12)}$$

For surface points, eqs A6 and A9 become

$$\frac{1}{2}\psi(\mathbf{s}_0) = v^e(\mathbf{s}_0) - \int_S F(\alpha,\mathbf{x},\mathbf{s}_0)p^e(\mathbf{x})\,\mathrm{d}S_x + \int_S F'(\alpha,\mathbf{x},\mathbf{s}_0)\psi(\mathbf{x})\,\mathrm{d}S_x \quad \text{(A13)}$$

$$\frac{1}{2}\psi(\mathbf{s}_0) = v^i(\mathbf{s}_0) + \int_S F(0,\mathbf{x},\mathbf{s}_0)p^i(\mathbf{x})\,\mathrm{d}S_x - \int_S F'(0,\mathbf{x},\mathbf{s}_0)\psi(\mathbf{x})\,\mathrm{d}S_x \quad \text{(A14)}$$

where interior and exterior source terms have been introduced

$$v^i(\mathbf{s}) = -\int_{V_i} F(0,\mathbf{x},\mathbf{s})h(0,\mathbf{x})\,\mathrm{d}V_x \quad \text{(A15)}$$

$$v^e(\mathbf{s}) = -\int_V F(\alpha,\mathbf{x},\mathbf{s})h(\alpha,\mathbf{x})\,\mathrm{d}V_x \quad \text{(A16)}$$

In numerical applications, it is convenient to break the polyion surface into N triangular platelets and the exterior volume into M volume elements. In principle, the exterior volume is unbounded but the integrand of eq A16 is only significant near the polyion surface. Thus, it is possible to truncate the exterior volume to a good approximation. The interior volume integral in eq A15 can be replaced with a discrete sum of terms in the applications considered in this work so the integral does not have to be evaluated as written. Within the surface/volume elements, ψ, p^e, p^i, and h are assumed constant but the integrals over F and F' are evaluated numerically. It is convenient to define the following integrals

$$I_1(\alpha,k,\mathbf{s}) = -\int_{S_k} F'(\alpha,\mathbf{x},\mathbf{s})\,\mathrm{d}S_x \quad \text{(A17)}$$

$$I_2(\alpha,k,\mathbf{s}) = \int_{S_k} F(\alpha,\mathbf{x},\mathbf{s})\, \mathrm{d}S_x \qquad \text{(A18)}$$

$$I_v(\alpha,l,\mathbf{s}) = \int_{V_l} F(\alpha,\mathbf{x},\mathbf{s})\, \mathrm{d}V_x \qquad \text{(A19)}$$

where k/l refers to the kth surface/lth volume element. The normal derivative is

$$F'(\alpha,\mathbf{x},\mathbf{s}) = -\frac{(1+\alpha y)\mathrm{e}^{-\alpha y}\mathbf{n}\cdot\mathbf{y}}{4\pi y^3} \qquad \text{(A20)}$$

where $y = |\mathbf{y}| = |\mathbf{x} - \mathbf{s}|$.

In addition to the potential, ψ, we shall need gradients in ψ as well. For this reason, it is convenient to define some additional integrals

$$\mathbf{H}_1(\alpha,k,\mathbf{s}) = -\int_{S_k} \nabla_s F'(\alpha,\mathbf{x},\mathbf{s})\, \mathrm{d}S_x \qquad \text{(A21)}$$

$$\mathbf{H}_2(\alpha,k,\mathbf{s}) = \int_{S_k} \nabla_s F(\alpha,\mathbf{x},\mathbf{s})\, \mathrm{d}S_x \qquad \text{(A22)}$$

$$\mathbf{H}_v(\alpha,l,\mathbf{s}) = \int_{V_l} \nabla_s F(\alpha,\mathbf{x},\mathbf{s})\, \mathrm{d}V_x \qquad \text{(A23)}$$

and

$$\nabla_s F = \frac{\mathrm{e}^{-\alpha y}}{4\pi y^3}(1+\alpha y)\mathbf{y} \qquad \text{(A24)}$$

$$\nabla_s F' = \frac{\mathrm{e}^{-\alpha y}}{4\pi y^3}\left[(1+\alpha y)\mathbf{n} - \left(\alpha^2 + \frac{3(1+\alpha y)}{y^2}\right)(\mathbf{n}\cdot\mathbf{y})\mathbf{y}\right] \qquad \text{(A25)}$$

Now let ψ_j denote the surface potential on platelet j (centered at $\mathbf{s}_j$) and use similar notation for the p's and v's. Discretizing eqs A13 and A14 using the above definitions yields

$$\frac{1}{2}\psi_j = v_j^{\mathrm{e}} - \sum_k I_2(\alpha,k,\mathbf{s}_j)p_k^{\mathrm{e}} - \sum_k I_1(\alpha,k,\mathbf{s}_j)\psi_k \qquad \text{(A26)}$$

$$\frac{1}{2}\psi_j = v_j^{\mathrm{i}} + \sum_k I_2(0,k,\mathbf{s}_j)p_k^{\mathrm{i}} + \sum_k I_1(0,k,\mathbf{s}_j)\psi_k \qquad \text{(A27)}$$

As discussed in the main part of this paper, solution of eqs A26 and A27 for ψ and p in the case of Poisson equations or simply eq A26 in the case of the ion transport equation allows subsequent determination of $\psi(\mathbf{s})$ for any field point. Discretizing eq A6 for exterior points

$$\psi(\mathbf{s}) = v^{\mathrm{e}}(\mathbf{s}) - \sum_k I_2(\alpha,k,\mathbf{s})p_k^{\mathrm{e}} - \sum_k I_1(\alpha,k,\mathbf{s})\psi_k \qquad \text{(A28)}$$

$$v^{\mathrm{e}}(\mathbf{s}) = -\sum_l I_v(\alpha,l,\mathbf{s})h_l(\alpha) \qquad \text{(A29)}$$

where $h_l(\alpha) = h(\alpha,\mathbf{x}_l)$ and $\mathbf{x}_l$ is the center point position for volume element l. The corresponding gradient is

$$\nabla\psi(\mathbf{s}) = \nabla v^{\mathrm{e}}(\mathbf{s}) - \sum_k \mathbf{H}_2(\alpha,k,\mathbf{s})p_k^{\mathrm{e}} - \sum_k \mathbf{H}_1(\alpha,k,\mathbf{s})\psi_k \qquad \text{(A30)}$$

$$\nabla v^{\mathrm{e}}(\mathbf{s}) = -\sum_l \mathbf{H}_v(\alpha,l,\mathbf{s})h_l(\alpha) \qquad \text{(A31)}$$

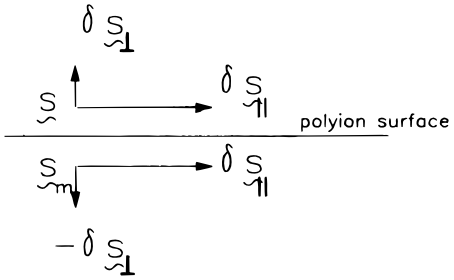

Figure 5. Schematic of **s** and its mirror point near the polyion surface. Also depicted are the corresponding tangential and normal displacements.

A common problem in BE methods[23−25] is that ψ and, to an even greater extent, $\nabla\psi$ become difficult to compute numerically for field points near the polyion surface. This is related to the discontinuous nature of I_1 (see eqs A11, A12, and A17). Error can be reduced[38] by considering a corresponding mirror point, $\mathbf{s}_m$, just inside the polyion surface, as shown in Figure 5. Discretizing eq A10, we have

$$0 = v^{\mathrm{e}}(\mathbf{s}_m) - \sum_k I_2(\alpha,k,\mathbf{s}_m)p_k^{\mathrm{e}} - \sum_k I_1(\alpha,k,\mathbf{s}_m)\psi_k \qquad \text{(A32)}$$

Now if we add eqs A28 and A32, we expect the discontinuities in I_1 from the **s** and $\mathbf{s}_m$ terms to cancel each other on the basis of eqs A11 and A12

$$\psi(\mathbf{s}) = v^{\mathrm{e}}(\mathbf{s}) + v^{\mathrm{e}}(\mathbf{s}_m) - \sum_k (I_2(\alpha,k,\mathbf{s}) + I_2(\alpha,k,\mathbf{s}_m))p_k^{\mathrm{e}} - \sum_k (I_1(\alpha,k,\mathbf{s}) + I_1(\alpha,k,\mathbf{s}_m))\psi_k \qquad \text{(A33)}$$

Before discussing the gradient in ψ near the surface, it will be helpful to introduce

$$\boldsymbol{\chi}_1 = \nabla v^{\mathrm{e}}(\mathbf{s}) + \nabla v^{\mathrm{e}}(\mathbf{s}_m) - \sum_k (\mathbf{H}_2(\alpha,k,\mathbf{s}) + \mathbf{H}_2(\alpha,k,\mathbf{s}_m))p_k^{\mathrm{e}} - \sum_k (\mathbf{H}_1(\alpha,k,s) + \mathbf{H}_1(\alpha,k,\mathbf{s}_m))\psi_k \qquad \text{(A34)}$$

$$\boldsymbol{\chi}_2 = \nabla v^{\mathrm{e}}(\mathbf{s}) - \nabla v^{\mathrm{e}}(\mathbf{s}_m) - \sum_k (\mathbf{H}_2(\alpha,k,\mathbf{s}) - \mathbf{H}_2(\alpha,k,\mathbf{s}_m))p_k^{\mathrm{e}} - \sum_k (\mathbf{H}_1(\alpha,k,\mathbf{s}) - \mathbf{H}_1(\alpha,k,\mathbf{s}_m))\psi_k \qquad \text{(A35)}$$

where $\boldsymbol{\chi}_1$ corresponds to adding the gradients of eqs A28 and A32 and $\boldsymbol{\chi}_2$ corresponds to subtracting them. Which one is appropriate depends on whether or not the gradient is tangential or normal to the polyion surface. Consider first the tangential gradient. A particular component of the tangential gradient can be obtained from the change in ψ on going from **s** to $\mathbf{s} + \delta\mathbf{s}_{\parallel}$, as illustrated in Figure 5. Near the surface eq A33 should be used to estimate the potential at both **s** and $\mathbf{s}_m$. Since $\delta\mathbf{s}_{\parallel}$ is the same for both **s** and $\mathbf{s}_m$, eq A34 is appropriate for the tangential component. The normal gradient, however, must be handled differently since $\delta\mathbf{s}_{\perp}$ for the mirror point is of opposite sign from the field point (Figure 5). Consequently, eq A35 is appropriate for the normal gradient. Overall, this can be handled by writing

$$\nabla\psi(\mathbf{s}) = (\boldsymbol{\chi}_1 - \mathbf{n}(\mathbf{n}\cdot\boldsymbol{\chi}_1)) + \mathbf{n}(\mathbf{n}\cdot\boldsymbol{\chi}_2) \qquad \text{(A36)}$$

In this work the volume sorrounding the polyion is broken up into shells which conform to the surface of

the polyion. Shell 1, for example, occupies a thin layer adjacent to the polyion surface. Each shell, in turn, is divided into N additional volume elements (N is the number of surface platelets). In this work, eq A36 is used for the innermost four shells and eq A30 is used in outer shells. In the case of the ion relaxation problem, the normal component is handled differently for the innermost shells, as discussed in the main part of this paper.

The integrals defined by eqs A17−A19, and A21−A23 are solved numerically by several different methods. For large y (greater than several nanometers) the integrand is evaluated at a single point. For smaller y, they are either solved by iterative methods or by a Monte Carlo procedure. In the iterative method, the surface or volume is divided into successively finer arrays of elements and the integral evaluated as a sum over these elements. The iteration is continued until the integral converges to within some tolerance level (typically 0.01). In the Monte Carlo method, some number (typically 100) of points are selected at random from the surface or volume element and the integrand average is determined. The integral is approximated as the integrand average times the appropriate area or volume. When the field point falls within, on, directly above, or below the surface or volume element, part of the integral (a circular patch or disk containing the field point) can be solved analytically. In those cases, part of the integral is solved analytically and the remainder numerically. All procedures have been thoroughly tested.

References and Notes

(1) Overbeek, J. Th. G. In *Electrophoresis*; Beer, M., Ed.; Academic: New York, 1967; Vol. 2, Chapter 1.
(2) Hunter, R. J. *Zeta Potential in Colloid Science*; Academic: New York, 1981.
(3) Dukhin, S. S.; Shilov, V. N. *Dielectric Phenomena and the Double Layer in Disperse Systems and Polyelectrolytes*; John Wiley & Sons: New York, 1974.
(4) Anderson, J. L. *Annu. Rev. Fluid Mech.* **1989**, *21*, 61.
(5) Anderson, J. L. *J. Colloid Interface Sci.* **1985**, *105*, 45.
(6) Fair, M. C.; Anderson, J. L. *J. Colloid Interface Sci.* **1989**, *127*, 388.
(7) O'Brien, R. W. *J. Colloid Interface Sci.* **1983**, *92*, 204.
(8) Solomentsev, Y. E.; Pawar, Y.; Anderson, J. L. *J. Colloid Interface Sci.* **1993**, *158*, 1.
(9) Fair, M. C.; Anderson, J. L. *Langmuir* **1992**, *8*, 2850.
(10) Henry, D. C. *Proc. R. Soc. London, Ser. A* **1931**, *133*, 106.
(11) Overbeek, J. Th. G. In *Advances in Colloid Science*; Mark, H., Ed.; Interscience Publishing: New York, 1950; Vol. 3.
(12) Booth, F. *Proc. R. Soc. London, Ser. A* **1950**, *203*, 514.
(13) Wiersema, P. H. On the Theory of Electrophoresis. Ph.D. Thesis, Utrecht University, Utrecht, The Netherlands, 1964.
(14) Wiersema, P. H.; Loeb, A. L.; Overbeek, J. Th. G. *J. Colloid Interface Sci.* **1966**, *22*, 78.
(15) O'Brien, R. W.; White, L. R. *J. Chem. Soc., Faraday Trans. 2* **1978**, *74*, 1607.
(16) Schellman, J. A.; Stigter, D. *Biopolymers* **1977**, *16*, 1415.
(17) Allison, S. A.; Tran, V. T. *Biophys. J.* **1995**, *68*, 2261.
(18) Allison, S. A.; Bacquet, R. J.; McCammon, J. A. *Biopolymers* **1988**, *27*, 251.
(19) Chae, K. S.; Lenhoff, A. M. *Biophys. J.* **1995**, *68*, 1120.
(20) Allison, S. A.; Nambi, P. *Macromolecules* **1994**, *27*, 1413.
(21) Teubner, M. *J. Chem. Phys.* **1982**, *76*, 5564.
(22) Zhou, H.-X. *J. Chem. Phys.* **1994**, *100*, 3152.
(23) Yoon, B. J.; Lenhoff, A. M. *J. Comput. Chem.* **1990**, *11*, 1080.
(24) Juffer, A. H.; Botta, E. F. F.; Van Keulen, B. A. M.; Van Der Ploeg, A.; Berendsen, H. J. C. *J. Comput. Phys.* **1991**, *97*, 144.
(25) Zhou, H.-X. *Biophys. J.* **1993**, *65*, 955.
(26) Allison, S. A.; Nambi, P. *Macromomolecules* **1992**, *25*, 3971.
(27) Pakdel, P.; Kim, S. *J. Rheol.* **1991**, *35*, 797.
(28) Loeb, A. L.; Overbeek, J. Th. G.; Wiersema, P. H. *The Electric Double Layer Around a Spherical Colloid Particle*; MIT Press: Cambridge, MA, 1961.
(29) Fixman, M.; Jagannathan. *J. Chem. Phys.* **1981**, *75*, 4048.
(30) Yoon, B. J. *J. Colloid Interface Sci.* **1991**, *142*, 575.
(31) Fixman, M. *J. Chem. Phys.* **1979**, *70*, 4995.
(32) LeBret, M.; Zimm, B. H. *Biopolymers* **1984**, *23*, 270.
(33) Murthy, C. S.; Bacquet, R. J.; Rossky, P. O. *J. Phys. Chem.* **1985**, *89*, 701.
(34) Mills, P.; Anderson, C. F.; Record, M. T. *J. Phys. Chem.* **1985**, *89*, 3984.
(35) Henderson, D.; Blum, L. *J. Chem. Phys.* **1978**, *69*, 5441.
(36) Fuoss, R. M.; Onsager, L. *J. Phys. Chem.* **1957**, *61*, 668.
(37) Grycuk, T.; Antosiewicz, J.; Porschke, D. *J. Phys. Chem.* **1994**, *98*, 10881.
(38) Liu, Y. J.; Zhang, M.; Rizzo, F. J. In *Boundary Elements XV, Vol. 1. Fluid Flow and Computational Aspects*; Brebbia, C. A., Rencis, J. J., Eds.; Computational Mechanics Publishers: Boston, 1993; p 453.

MA960890W